



# Three-Dimensional Neutronics Analysis for the US Magnet Shield of ITER

M.E. Sawan and L.A. El-Guebaly

October 1990

UWFDM-838

Presented at the 9th Topical Meeting on the Technology of Fusion Energy, 7–11 October 1990, Oak Brook IL; Fusion Tech. 19 (1991) 1469.

***FUSION TECHNOLOGY INSTITUTE***

***UNIVERSITY OF WISCONSIN***

***MADISON WISCONSIN***

### **DISCLAIMER**

This report was prepared as an account of work sponsored by an agency of the United States Government. Neither the United States Government, nor any agency thereof, nor any of their employees, makes any warranty, express or implied, or assumes any legal liability or responsibility for the accuracy, completeness, or usefulness of any information, apparatus, product, or process disclosed, or represents that its use would not infringe privately owned rights. Reference herein to any specific commercial product, process, or service by trade name, trademark, manufacturer, or otherwise, does not necessarily constitute or imply its endorsement, recommendation, or favoring by the United States Government or any agency thereof. The views and opinions of authors expressed herein do not necessarily state or reflect those of the United States Government or any agency thereof.

# **Three-Dimensional Neutronics Analysis for the US Magnet Shield of ITER**

M.E. Sawan and L.A. El-Guebaly

Fusion Technology Institute  
University of Wisconsin  
1500 Engineering Drive  
Madison, WI 53706

<http://fti.neep.wisc.edu>

October 1990

UWFDM-838

Presented at the 9th Topical Meeting on the Technology of Fusion Energy, 7–11 October 1990, Oak Brook IL; Fusion Tech. 19 (1991) 1469.

# THREE-DIMENSIONAL NEUTRONICS ANALYSIS FOR THE U.S. MAGNET SHIELD OF ITER

M.E. Sawan and L.A. El-Guebaly  
Fusion Technology Institute  
University of Wisconsin-Madison  
1500 Johnson Drive  
Madison, WI 53706  
(608) 263-5093

## ABSTRACT

Detailed three-dimensional neutronics calculations have been performed for the U.S. design of the ITER magnet shield. The total nuclear heating in the TF coils is 35 kW in the technology phase and 42 kW in the physics phase. Using 5 cm thick W back shield layers behind the vacuum vessel in locations with limited shielding space results in acceptable local magnet damage levels. The parts of the TF coils adjacent to the divertor vacuum pumping ducts are well protected against streaming radiation.

## INTRODUCTION

The prime function of the bulk shield in the International Thermonuclear Experimental Reactor (ITER) is to provide adequate protection for the toroidal field (TF) coils. The ITER reactor operates in two phases. The physics phase operation corresponds to 0.05 full power years (FPY) at a fusion power of 1100 MW and is followed by a 3.8 FPY technology phase at 860 MW of fusion power. The design limits for magnet radiation effects are  $5 \times 10^9$  rads, 65 kW, 5 mW/cm<sup>3</sup> and  $10^{19}$  n/cm<sup>2</sup> for the peak insulator dose, total nuclear heating, peak nuclear heating in the winding pack, and peak fast neutron fluence ( $E > 0.1$  MeV). In addition helium production in the vacuum vessel (V.V.) is limited to 0.1 appm for reliable rewelding.

Due to the geometrical complexity of the shield configuration in ITER, three-dimensional (3-D) models are required to properly determine the magnet radiation effects. In this work, detailed three-dimensional neutronics calculations have been performed to determine the total nuclear heating in the TF coils as well as the contributions from the different parts of the inboard and divertor regions. The 3-D calculations are aimed also at calculating the end of life magnet radiation effects in areas with critical shielding space. Two sets of calculations that complement each other have been performed. In the first calculation, the lower part of the reactor was modeled in detail to determine the radiation effects in parts of the TF coils adjacent to the vacuum pumping ducts and divertor coolant tubes. In the second calculation, the upper part of the reactor was modeled with detailed magnet configuration in the inboard,

outboard, and upper divertor regions. The total nuclear heating was then determined by adding the results of the two sets of calculations. Finally, the results of the 3-D analysis will be compared to the 1-D results.<sup>1</sup>

## 3-D ANALYSIS FOR THE LOWER DIVERTOR REGION

### Calculational Model

Detailed three-dimensional neutronics calculations have been performed to determine the radiation effects in the parts of the TF coils behind the lower divertor region and adjacent to the vacuum pumping ducts. The continuous energy, coupled neutron-gamma-ray Monte Carlo code MCNP, version 3B,<sup>2</sup> has been used in the calculations. Because of symmetry, only 1/64 of the reactor was modeled with surrounding reflecting boundaries. Detailed configurations of the blanket, shield, V.V., coil case (C.C.), and winding pack (W.P.) in the divertor region were included in the model. In addition, the divertor plates, vacuum pumping ducts and divertor coolant tubes penetrating between TF coils were modeled in detail.

Figures 1, 2, and 3 show vertical cross sections of the geometrical model used at toroidal locations through the vacuum pumping duct, the divertor coolant tubes, and the TF coil, respectively. The magnet in the divertor region was divided into four zones as indicated in Figure 3. Tungsten is used in the 5 cm thick back layer outside the V.V. in Zones II and III where the shielding space is limited and B<sub>4</sub>C/Pb shield is used as a back layer in Zones I and IV. The smallest shield/V.V. thickness is 47 cm at the edge of the divertor plate. Horizontal cross sections at different vertical locations are given in Figure 4. At the side of the vacuum pumping duct the shield thickness is 30 cm and the V.V. thickness is 10 cm. The 2-cm-wide assembly gaps between adjacent blanket/shield modules are included in the model. 316 SS/H<sub>2</sub>O (at 20 vol.% H<sub>2</sub>O) is used in the bulk and penetration shield.

Seventy thousand source particles have been sampled in the MCNP calculation. The neutron source was sampled

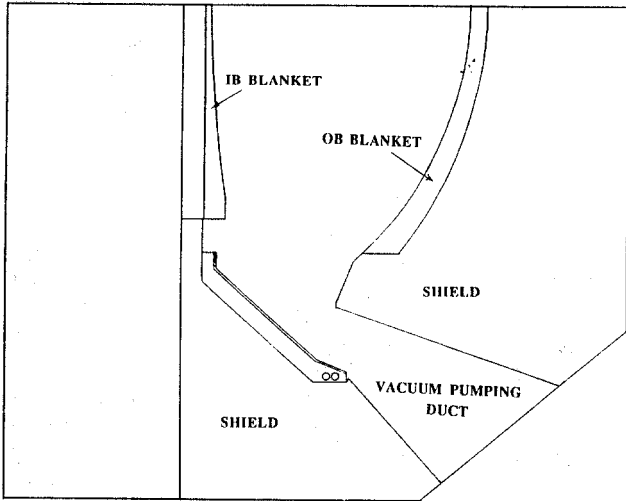


Figure 1. Vertical cross section through the vacuum pumping duct.

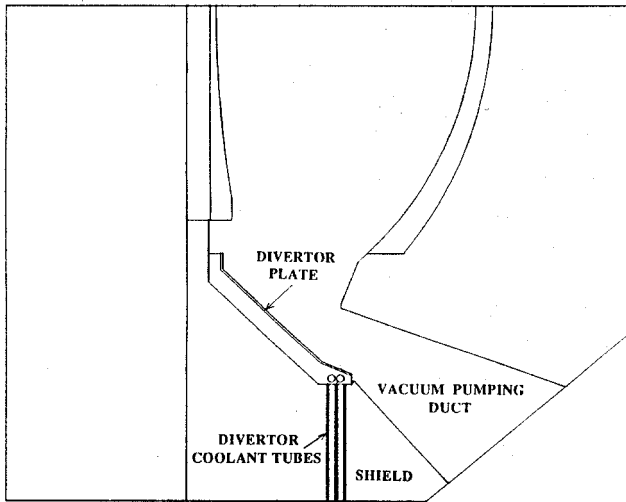


Figure 2. Vertical cross section through the divertor coolant tubes.

from the actual source profile in the D-shaped plasma. Angular source biasing was used to improve the accuracy of the calculated magnet radiation effects in the lower divertor region. In addition, geometry splitting and weight cutoff with Russian roulette techniques were used for variance reduction. Continuous energy cross section data were used for the MCNP calculation. The ENDF/B-V, revision 2 evaluation was used for all nuclides except for Sn where the ENDL-1985 evaluation was used. Surface flux tallies were used to determine the radiation effects at the front and side surfaces of the TF coils. The results were normalized to the technology phase fusion power of 860 MW. The end of life fluence related radiation effects were determined for 3.8 FPY of operation which is equivalent to the ITER fluence goal of  $3 \text{ MW}\cdot\text{y}/\text{m}^2$ .

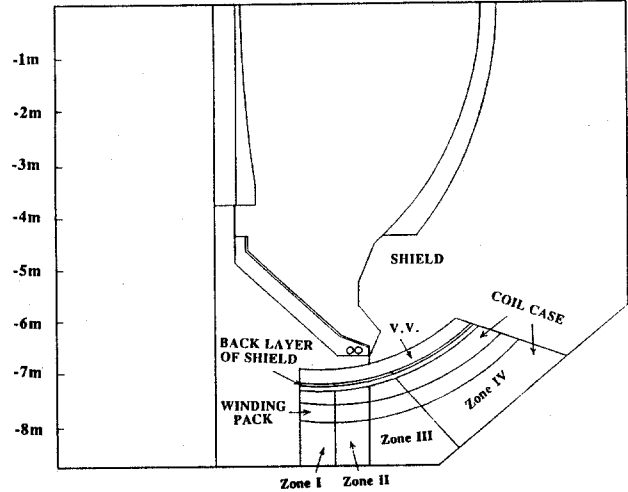
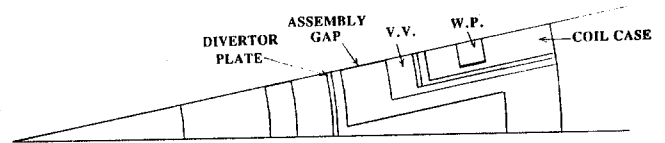
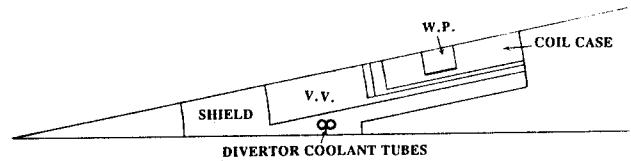


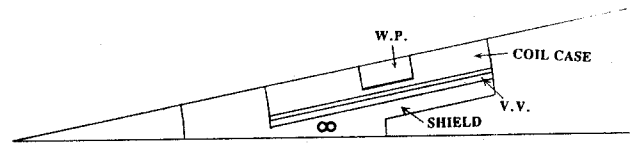
Figure 3. Vertical cross section through the TF coil.



**HORIZONTAL CROSS SECTION AT Z=-6.5m**



**HORIZONTAL CROSS SECTION AT Z=-7m**



**HORIZONTAL CROSS SECTION AT Z=-7.5m**

Figure 4. Horizontal cross sections of the model at different vertical locations.

Table 1. Peak End of Life Radiation Effects in W.P. in the Lower Divertor Region.

Zone	Insulator Dose (rads)		Fast Neutron Fluence (n/cm <sup>2</sup> )	
	Front	Side	Front	Side
Zone I	$4.35 \times 10^8$ (.18)	$2.94 \times 10^8$ (.21)	$7.77 \times 10^{17}$ (.10)	$6.93 \times 10^{17}$ (.22)
Zone II	$1.82 \times 10^9$ (.15)	$7.82 \times 10^8$ (.19)	$2.89 \times 10^{18}$ (.08)	$1.15 \times 10^{18}$ (.17)
Zone III	$1.79 \times 10^9$ (.15)	$7.20 \times 10^8$ (.28)	$2.42 \times 10^{18}$ (.12)	$1.05 \times 10^{18}$ (.15)
Zone IV	$5.92 \times 10^7$ (.22)	$3.96 \times 10^7$ (.26)	$1.10 \times 10^{17}$ (.22)	$8.79 \times 10^{16}$ (.27)

Neutron Streaming Through Divertor Vacuum Pumping Ducts

Neutrons crossing surface detectors at the entrance, sides, and exit of the vacuum pumping duct were tallied to quantify neutrons streaming into the divertor vacuum pumping ducts. The results indicate that  $2.82 \times 10^{-4}$  ( $\pm 3\%$ ) neutrons stream into each vacuum pumping duct per DT fusion. The number in parentheses corresponds to the statistical uncertainty in the Monte Carlo calculation. 10.5% of these neutrons are uncollided source neutrons streaming directly into the duct. The number of neutrons incident on both sides of the duct per DT fusion is  $3.38 \times 10^{-5}$  ( $\pm 6\%$ ),  $1.96 \times 10^{-5}$  ( $\pm 8\%$ ), and  $2.76 \times 10^{-5}$  ( $\pm 8\%$ ) for segments adjacent to the inner C.C., the W.P., and the outer C.C., respectively. The fractions of these neutrons coming directly from the source are 2%, 0.1%, and 0%, respectively. The leakage out of the vacuum pumping duct at the back of the C.C. is a very soft spectrum and amounts to  $7.75 \times 10^{-5}$  ( $\pm 4\%$ ) neutrons per DT fusion. The total number of neutrons leaking from the 16 vacuum pumping ducts is  $1.24 \times 10^{-3}$  per DT fusion. This amounts to  $3.78 \times 10^{17}$  neutrons per second in the technology phase.

Magnet Radiation Effects in the Lower Divertor Region

The end of life insulator dose and fast neutron fluence ( $E > 0.1$  MeV) averaged over the front and side surfaces of the W.P. in the four zones of the TF coil are given in Table 1. Values in parentheses correspond to the statistical uncertainty in the estimate of the response. It is clear that the sides of the coils are well protected from neutrons streaming into the vacuum pumping ducts and divertor coolant tubes. In all zones, the highest radiation effects occur at the front surface of the coil. The largest radiation effects are in Zones II and III because the shield is thinner at the edge of the divertor plate. The values of the insulator dose and fast neutron fluence are acceptable even when a 1.5 safety factor is included to account for nuclear data and modeling uncertainties. The end of life helium production at the inner surface of the V.V. has been determined to be 0.45, 5.58, 2.30, and 0.11 appm in Zones I, II, III, and IV, respectively. This indicates that the 0.1 appm limit required for rewelding is exceeded and rewelding should be avoided in these zones. Table 2 gives

the total nuclear heating in the lower parts of the sixteen TF coils for the technology phase. Again, Zones II and III with the smallest shield thickness give the largest contribution to the nuclear heating. In the physics phase, the nuclear heating increases by 28% due to the larger fusion power.

Table 2. Nuclear Heating (kW) in the Lower Parts of the 16 TF Coils for the Technology Phase.

Zone	W.P.	C.C.	Total
Zone I	0.27 (.09)	1.13 (.07)	1.40 (.06)
Zone II	0.73 (.07)	4.14 (.05)	4.87 (.05)
Zone III	0.70 (.09)	3.66 (.07)	4.36 (.06)
Zone IV	0.09 (.22)	0.90 (.14)	0.99 (.12)
Total	1.79 (.07)	9.83 (.05)	11.62 (.05)

3-D ANALYSIS FOR THE UPPER PART OF THE REACTOR

Calculational Model

The upper part of ITER was modeled for the Monte Carlo code MCNP.<sup>2</sup> Due to symmetry, 1/64 of the reactor was modeled with reflecting boundaries. The detailed configuration of the blanket, shield, V.V., C.C., W.P. and divertor plates was included in the model. The poloidally varying blanket thickness, the layered inboard shield, and the 2 cm wide assembly gaps were modeled in detail. 100,000 source particles were sampled using the actual source profile in the D-shaped toroidal plasma. The magnet was divided into 6 segments in the inboard region, 6 segments in the divertor region and 3 segments in the outboard region to determine the poloidal profiles of the magnet radiation effects. The magnet segments are indicated in Figure 5 which gives a vertical cross section of the geometrical model used in the calculations. Horizontal cross sections of the model are shown in Figure 6. B<sub>4</sub>C/Pb shield is used in the 5 cm thick back layer outside the V.V. in all regions except in regions II, D4 and D5 where W is used because of the limited shielding space. Variance reduction techniques including geometry splitting

and weight cutoff with Russian roulette were used in the calculations. Surface flux tallies were used to determine the peak radiation effects at the inner surface of the TF coils. The results were normalized to the technology phase fusion power of 860 MW and the reactor lifetime of 3.8 FPY corresponding to the ITER fluence goal of  $3 \text{ MW}\cdot\text{y}/\text{m}^2$ .

### Magnet Radiation Effects

The radiation effects at the inner surface of the W.P. are given in Table 3 for the different segments of the TF coils in the inboard and upper divertor regions. Because of the thick outboard blanket and shield, only a few particles reached the TF coil in the outboard region in the calculation with 100,000 histories yielding results with large statistical uncertainties. The 1-D neutronics analysis indicated that the peak outboard magnet radiation effects are about 5 orders of magnitude less than those in the inboard region with negligible contribution ( $< 0.1\%$ ) to the total magnet heating.<sup>1</sup> The results in Table 3 indicate that the peak end of life insulator dose and fast neutron fluence occur at the midplane in the inboard region. These values of  $2.77 \times 10^9$  rads and  $4.07 \times 10^{18} \text{ n/cm}^2$  are below the design limits of  $5 \times 10^9$  rads and  $10^{19} \text{ n/cm}^2$  even when a 1.5 safety factor is included to account for nuclear data and modeling uncertainties. The largest magnet radiation effects in the upper divertor region are in parts of the coil behind the outer end of the divertor plates (segments D4 and D5). Slightly higher values were obtained in the lower divertor region due to the presence of the vacuum pumping ducts. The end of life helium production at the inner surface of the V.V. was also determined for the different poloidal regions. The peak in the inboard region at the midplane is 0.8 appm and the peak in the divertor region is 7.2 appm. The results indicate that the helium production limit of 0.1 appm in the V.V. required for rewelding is exceeded everywhere except behind the middle part of the divertor plate and in the outboard region. Table 4 gives the total nuclear heating in the upper half of the 16 TF coils for the technology phase. Notice that while the C.C. contribution is less than that of the W.P. in the inboard region, magnet nuclear heating in the divertor region is dominated by the C.C. because of the fairly thick C.C.

### TOTAL NUCLEAR HEATING IN THE TF COILS

The nuclear heating values in the lower half are considered to be the same as in the upper half for all regions except for segments D3, D4, D5, and D6 where results of the calculation for the lower divertor region are used. Combining the results for the upper and lower halves of the coils, the total nuclear heating in the 16 TF coils is 34.5 kW in the technology phase and 42.2 kW in the physics phase. The additional 2 cm graphite tiles used in the inboard region during the physics phase result in reducing the magnet heating. However, the larger fusion power in the physics phase yields a net increase in magnet heating. These values are below the design limit of 65 kW even when a safety factor is included to account for nuclear data and modeling uncertainties. Nuclear heating in the

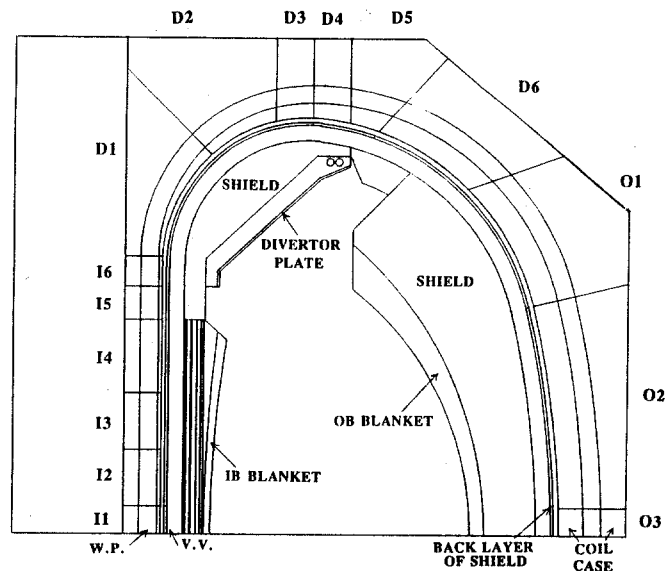
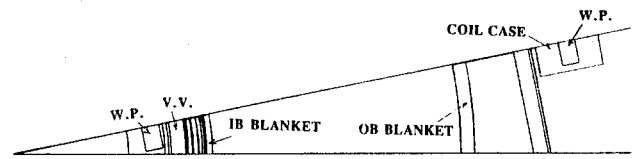


Figure 5. Vertical cross section of the geometrical model for the upper part of the reactor.



### HORIZONTAL CROSS SECTION AT MIDPLANE

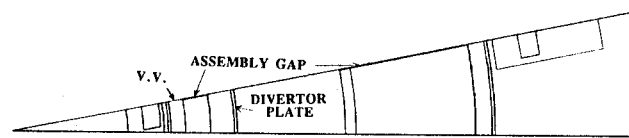


Figure 6. Horizontal cross sections of the geometrical model.

other reactor regions was also calculated. In the technology phase, values for nuclear heating in the inboard blanket, inboard shield, outboard blanket, outboard shield, divertor plates, divertor shield, and vacuum vessel are 107, 90, 613, 111, 22, 123, and 4 MW, respectively.

### COMPARISON WITH 1-D RESULTS

It is interesting to compare the results of the 1-D and 3-D analyses. The calculated nuclear heating, insulator dose, and He production in the V.V. are listed in Table 5. The values computed by either the 1-D or 3-D code are given followed by the values including the safety factors considered in the study. These safety factors are 3 and 2 for the local and integrated 1-D results and 1.5 and 1.4 for

Table 3. Radiation Effects at Inner Surface of W.P. in the Upper Parts of the TF Coils.

Region	Insulator Dose (rads)	Fast n Fluence (n/cm <sup>2</sup> )	Power Density (mW/cm <sup>3</sup> )
<u>Inboard</u>			
I1	$2.77 \times 10^9$ (.09)	$4.07 \times 10^{18}$ (.08)	0.61 (.10)
I2	$2.39 \times 10^9$ (.06)	$3.35 \times 10^{18}$ (.07)	0.55 (.08)
I3	$1.28 \times 10^9$ (.20)	$1.75 \times 10^{18}$ (.17)	0.29 (.20)
I4	$3.08 \times 10^8$ (.14)	$4.46 \times 10^{17}$ (.14)	0.08 (.14)
I5	$9.25 \times 10^8$ (.12)	$1.39 \times 10^{18}$ (.11)	0.20 (.14)
I6	$1.17 \times 10^9$ (.12)	$1.80 \times 10^{18}$ (.11)	0.24 (.13)
<u>Divertor</u>			
D1	$1.88 \times 10^8$ (.12)	$3.47 \times 10^{17}$ (.11)	0.04 (.13)
D2	$2.96 \times 10^7$ (.19)	$4.99 \times 10^{16}$ (.23)	0.01 (.20)
D3	$5.23 \times 10^8$ (.09)	$8.77 \times 10^{17}$ (.08)	0.13 (.10)
D4	$1.75 \times 10^9$ (.05)	$2.87 \times 10^{18}$ (.05)	0.44 (.06)
D5	$1.30 \times 10^9$ (.06)	$2.23 \times 10^{18}$ (.06)	0.33 (.07)
D6	$3.71 \times 10^7$ (.15)	$6.03 \times 10^{16}$ (.13)	0.01 (.15)

Table 4. Nuclear Heating (kW) in the Upper Parts of the 16 TF Coils

Region	W.P.	Coil Case	Total
<u>Inboard</u>			
I1	0.64 (.07)	0.43 (.07)	1.07 (.07)
I2	1.07 (.06)	0.82 (.06)	1.89 (.06)
I3	0.55 (.17)	0.45 (.16)	1.00 (.16)
I4	0.20 (.12)	0.18 (.11)	0.38 (.11)
I5	0.28 (.10)	0.20 (.10)	0.48 (.10)
I6	0.28 (.10)	0.22 (.10)	0.50 (.10)
Total	3.02 (.07)	2.30 (.07)	5.32 (.06)
<u>Divertor</u>			
D1	0.25 (.11)	0.29 (.11)	0.54 (.11)
D2	0.04 (.17)	0.09 (.17)	0.13 (.17)
D3	0.21 (.07)	0.91 (.07)	1.12 (.07)
D4	0.62 (.05)	4.05 (.04)	4.67 (.04)
D5	0.66 (.05)	3.84 (.05)	4.50 (.05)
D6	0.04 (.11)	0.57 (.08)	0.61 (.08)
Total	1.82 (.05)	9.75 (.04)	11.57 (.04)

the local and integrated 3-D results, respectively. The major factors which cause the differences in the computed 1-D and 3-D results will be discussed shortly. Comparing the results with the safety factors reveals that while good agreement is obtained in the nuclear heating, the 1-D method tends to overestimate the local damage, particularly in the divertor region. The large difference in the local values (dose and He production) is attributed to the fact that the 3-D values are averaged over a surface (in order to

lower the statistical error) while the 1-D method yields peak local values.

Comparing the results of the 3-D calculation at the midplane of the inboard region to the results of the 1-D calculation<sup>1</sup> indicates that the peak insulator dose and power density in the W.P. are factors of 1.75 and 1.42 higher than the 1-D results, respectively. The radially integrated nuclear heating per unit height of the W.P. and C.C. are factors of 1.34 and 1.53 higher than the 1-D results, respectively. The differences between the 3-D and 1-D results are attributed to the differences in the calculational procedures used. These differences can be divided into two groups: codes and data differences and modeling differences. While the 1-D calculation uses the deterministic discrete ordinates code ONEDANT,<sup>3</sup> the 3-D calculation uses the Monte Carlo code MCNP with a statistical error associated with the results. While both calculations use the ENDF/B-V cross section data, MCNP uses continuous energy cross sections and ONEDANT uses multigroup cross sections with 46 neutron - 21 gamma groups. In addition, different codes were used to process the nuclear data.

The modeling of the reactor geometry is quite different in the two calculations. The actual source profile in the D-shaped toroidal plasma is used in the 3-D calculation while a uniform source in an infinitely extended cylindrical plasma is used in the 1-D calculation. As a result, for the same wall loading, the angular distribution of direct neutrons incident on the first wall is more peaked in the perpendicular direction in the 3-D model leading to more shield penetration and higher magnet damage. The detailed poloidal variations in geometry and material which



Table 5. Comparison Between 1-D and 3-D Results.

	Magnet Nuclear Heating in Technology Phase (kW)		Insulator Dose (10 <sup>9</sup> rads @ 3.8 FPY)		He Production in V.V. (appm @ 3.8 FPY)	
	1-D	3-D	1-D <sup>†</sup>	3-D <sup>‡</sup>	1-D <sup>†</sup>	3-D <sup>‡</sup>
Inner Legs	6/12	10.6/15.1	1.6/4.8	2.8/4.3	0.5/1.5	0.8/1.2
Upper Divertor	11/22	11.6/16.6	4.5/13.5	1.75/2.7	13.5/40	7.2/11
Lower Divertor and Penetrations	9.5*/19	12.3/17.6	3/9	1.82/2.8	6.4/19	5.6/8.6
Total Nuclear Heating:						
Technology Phase	26.5/53	34.5/49.3				
Physics Phase	33/66	42.2/60.3				

<sup>†</sup>Peak values

<sup>‡</sup>Average values over front surface of a zone

\*1.5 kW is added to account for penetrations

cannot be included in a 1-D model, are included in the 3-D calculation. This can lead to different results due to the strong neutronics coupling (reflection, spectral, and angular effects) between the different regions in the reactor. Furthermore, detailed toroidal variations in geometry and material, such as the assembly gap, the toroidally varying C.C. thickness, and the finite toroidal width of the W.P., are included in the 3-D model. These result in higher peak radiation effects in the W.P. and more contribution from the C.C. to the total heating. Other geometrical modeling differences include using a homogenized composition for the inboard and outboard blankets and the V.V. in the 3-D model.

## SUMMARY AND CONCLUSIONS

The 3-D neutronics analysis performed for the U.S. magnet shield design of ITER indicates that the parts of the TF coils adjacent to the lower divertor vacuum pumping ducts are well shielded against streaming radiation. The total nuclear heating in the 16 TF coils has been determined to be 35 kW in the technology phase and 42 kW in the physics phase. These values are below the 65 kW design limit even when uncertainties in nuclear data and modeling are taken into account. For the 3 MW·y/m<sup>2</sup> fluence goal, the peak insulator dose values in the inboard and divertor regions are  $2.8 \times 10^9$  and  $1.8 \times 10^9$  rads, respectively. The corresponding peak fast neutron fluence values are  $4.1 \times 10^{18}$  and  $2.9 \times 10^{18}$  n/cm<sup>2</sup>, respectively. These values are below the design limits of  $5 \times 10^9$  rads and  $10^{19}$  n/cm<sup>2</sup> even when safety factors are included to account for uncertainties in nuclear data and modeling.

Using W back shield layers behind the V.V. over a 1 m high inboard region at the midplane and behind the outer end of the divertor plate allowed the magnet radiation limits to be satisfied. Using B<sub>4</sub>C/Pb back layer instead of W in these regions results in ~20% increase in magnet

damage at these locations with critical shielding space. The end of life helium production in the vacuum vessel exceeds the 0.1 appm limit required for rewelding everywhere except behind the middle part of the divertor plate and in the outboard region. Different schemes other than welding need to be developed for assembling the vacuum vessel.

## ACKNOWLEDGEMENT

Funding for this work was provided by the U.S. Department of Energy.

## REFERENCES

1. L. EL-GUEBALY, "Overview of the U.S.-ITER Magnet Shield: Concepts and Problems," These Proceedings.
2. "MCNP - A General Monte Carlo Code for Neutron and Photon Transport, Version 3A," LA-7396-M, Rev. 2, Los Alamos National Laboratory (1986) and J. Briesmeister, "MCNP3B Newsletter," X-6-JFB-88-292, Los Alamos National Laboratory (July 1988).
3. R. O'DELL et al., "User's Manual for ONEDANT: A Code Package for One-Dimensional, Diffusion Accelerated, Neutral Particle Transport," LA-9184-M, Los Alamos National Laboratory (1982).